water

MDPI

Article

Incorporating Advanced Scatterometer Surface and Root Zone Soil Moisture Products into the Calibration of a Conceptual Semi-Distributed Hydrological Model

Martin Kubáň [1,*], Juraj Parajka [2,3], Rui Tong [2,3], Isabella Pfeil [2,4], Mariette Vreugdenhil [4], Patrik Sleziak [5], Brziak Adam [1], Ján Szolgay [1], Silvia Kohnová [1] and Kamila Hlavčová [1]

1 Department of Land and Water Resources Management, Slovak University of Technology, 81005 Bratislava, Slovakia; adam.brziak@stuba.sk (B.A.); jan.szolgay@stuba.sk (J.S.); silvia.kohnova@stuba.sk (S.K.); kamila.hlavcova@stuba.sk (K.H.)
2 Centre for Water Resource Systems, TU Wien, 1040 Vienna, Austria; parajka@hydro.tuwien.ac.at (J.P.); mrtongrui@gmail.com (R.T.); isabella.pfeil@geo.tuwien.ac.at (I.P.)
3 Institute of Hydraulic Engineering and Water Resources Management, TU Wien, 1040 Vienna, Austria
4 Department of Geodesy and Geoinformation, TU Wien, 1040 Vienna, Austria; Mariette.Vreugdenhil@geo.tuwien.ac.at
5 Institute of Hydrology, Slovak Academy of Sciences, Dúbravská Cesta 9, 84104 Bratislava, Slovakia; sleziak@uh.savba.sk
* Correspondence: martin.kuban@stuba.sk

Citation: Kubáň, M.; Parajka, J.; Tong, R.; Pfeil, I.; Vreugdenhil, M.; Sleziak, P.; Adam, B.; Szolgay, J.; Kohnová, S.; Hlavčová, K. Incorporating Advanced Scatterometer Surface and Root Zone Soil Moisture Products into the Calibration of a Conceptual Semi-Distributed Hydrological Model. *Water* **2021**, *13*, 3366. https://doi.org/10.3390/w13233366

Academic Editor: Aizhong Ye

Received: 12 October 2021
Accepted: 25 November 2021
Published: 28 November 2021

Abstract: The role of soil moisture is widely accepted as a significant factor in the mass and energy balance of catchments as a controller in surface and subsurface runoff generation. The paper examines the potential of a new dataset based on advanced scatterometer satellite remote sensing of soil moisture (ASCAT) for multiple objective calibrations of a dual-layer, conceptual, semi-distributed hydrological model. The surface and root zone soil moisture indexes based on ASCAT data were implemented into calibration of the hydrological model. Improvements not only in the instrument specifications, i.e., better temporal and spatial sampling, but also in the higher radiometric accuracy and retrieval algorithm, were applied. The analysis was performed in 209 catchments situated in different physiographic and climate zones of Austria for the period 2007–2018. We validated the model for two validation periods. The results show that multiple objective calibrations have a substantial positive effect on constraining the model parameters. The combined use of soil moisture and discharges in the calibration improved the soil moisture simulation in more than 73% of the catchments, except for the catchments with higher forest cover percentages. Improvements also occurred in the runoff model efficiency, in more than 27% of the catchments, mostly in the watersheds with a lower mean elevation and a higher proportion of farming land use, as well as in the Alpine catchments where the runoff is not significantly influenced by snowmelt and glacier runoff.

Keywords: ASCAT; semi-distributed hydrological model; surface soil moisture; root zone soil moisture; multiobjective calibration; HBV model

1. Introduction

Recently, various reviews have evaluated the hydrological aspects of using remotely-sensed soil moisture information. The potential of estimating soil moisture through remote sensing [1–6] and the use of satellite soil moisture data for climatic and hydrological uses was tackled in [7–11]. Numerical weather predictions, land surface and climate model assessments, monitoring of drouths, modelling of runoff, and forecasting of floods are the most critical applications that benefit from satellite soil moisture retrievals. No additional review of these aspects will be given here, nor will future opportunities be analyzed in this study. In the paper, we focus on the potential associated with using a particular remotely-sensed soil moisture product and its derivatives in rainfall runoff models. Recent advances

in the techniques of soil moisture observation, which were covered in [12], particularly remote sensing by passive and active microwaves, have increased the accessibility of soil moisture datasets both locally and regionally. That includes a new ASCAT Soil Water Index (SWI) data product.

It differs from the traditional ASCAT SWI operational product derived by the TU Wien Soil Moisture Retrieval approach [13], which the Copernicus Global Land Service distributes. This experimental SWI data product profits from a new vegetation parameterization used in the retrieval algorithm of the ASCAT surface soil moisture data [14]. It also includes a better spatial representation resulting from a new directional resampling method based on data from the Sentinel-1 Synthetic Aperture Radar (SAR) [12].

In rainfall-runoff modelling three main areas rely on the use of satellite data on soil moisture: antecedent soil moisture estimation for event-based rainfall-runoff model initializations (e.g., [15–18]), data assimilation for real time applications (e.g., [19–24]), and the multi-objective calibration of continuous hydrological models, which is the main topic of this paper. The rationale behind calibrating multi-objective hydrological models with ground data and satellite soil moisture data is that even though the models and data sources have clear limitations, they are not defined in exactly the same way. Their combination may therefore help reduce the uncertainties associated with estimates of catchment states and outputs.

Reduction in uncertainty and improvement of predictions in hydrological modelling by multiple objective calibrations that helped constrain hydrological models was demonstrated in many studies (for an overview, see, e.g., [25]). Many studies (such as [25–31]) have combined calibrating hydrological models to runoff and soil moisture variables. The usage of additional information usually resulted in improvements in representing the spatial and temporal patterns of the catchment's states and fluxes. However, that did not necessarily result in improving the efficiency of simulating runoff.

Generally speaking, these papers proved that using the scatterometer data for the model calibration can improve the match between the simulated and measured soil moisture in the conceptual and physically-based models.

A few studies also tested a combination of several variables in multiple objective calibrations [32–37] and determined that combining different data, particularly in data-poor regions, reduced the uncertainty in the model parameters in general. As shown in [35], the use of different soil moisture products had an interesting positive impact on the identifiability of the parameters of the snow module, too. However, based on its review of the scientific literature, [11] concluded that the conditions when benefits can be reached from the inclusion of information on satellite soil moisture to runoff modelling (both for data assimilation and model calibration) still need to be further clarified. While in some studies modest to noteworthy improvements through the inclusion of satellite data were reported, deterioration of the performances was often noted, too. These were related in [11] to the inherent uncertainty and problems associated with the use of satellite data (e.g., in the Soil Water Index method techniques [7]) and to the hydrological modelling itself. It was recommended to tailor the satellite data and request modelers to adapt models for the use of satellite data. This could include updating the model structure that mainly considers one soil storage element representing a single layer of soils and is often lumped spatially. This idea calls for an additional surface soil layer store representing the moisture close to the land surface and also considering spatially distributing soil properties. An increase in the spatial and temporal resolution of the satellite products was also called for. Long time series of soil moisture data (e.g., longer than ten to15 years) were recommended for use by hydrologists to evaluate the benefits of including such data in analyses [7].

This paper intends to respond to these conclusions and, in several ways, it goes beyond existing studies. In [12], the authors used the SWI ASCAT product of the root-zone soil moisture for the calibration of the TUW 15-parameter single soil layer model for the same Austrian catchments that we use for our work. In our paper, we use the SWI ASCAT root zone and SWI ASCAT surface moisture product. In the TUW model, 18 parameters (3 new

parameters for the surface layer) were considered for a dual soil layer structure. We also attempted to use a finer spatial resolution of the ASCAT product for both layers of the soil moisture estimates based on the data reported in [12]. A comparison of the soil moisture estimates was performed for different land uses and elevation zones, which allowed inferences to be made about the value of scatterometer data for hydrological modelling.

2. Materials

In this study, 209 Austrian catchments, based on a selection from previous studies such as [25,38], were used for the analysis. The catchments' areas vary between 13.7 (Micheldorf, Krems River,) to 6214 km^2 (Bruck an der Mur unter Muerz, Mur River) with a median of 167.3 km^2.The mean elevation varies between 353 to 2939 m a.s.l. with a median of 1010 m a.s.l. The percentage of the forest cover is between 0 and 94.6%, and the agricultural soil cover has a range from 0 up to 92.9%. The mean daily air temperature was between −2.83 °C for the Alpine catchments and up to 10.30 °C in the Lowland catchments. The location of the selected catchments is in Figure 1.

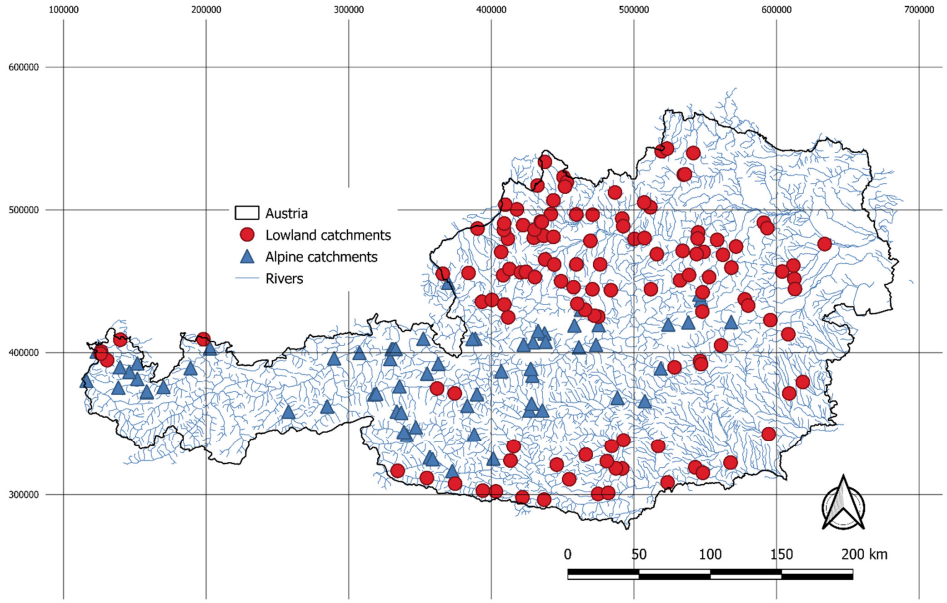

Figure 1. Location of the 209 Austrian catchments selected. The red dots denote the group of Lowland catchments and blue triangles the Alpine catchments.

The catchments' characteristics were obtained from various sources. The mean daily potential global solar radiation and morphology characteristics, i.e., elevations, roughness index, and slopes were derived from a digital elevation model of Austria. The sunshine index was estimated using the R.sun function in GIS-GRASS for 1 × 1 km^2 raster. Land use information was extracted from the Copernicus Land Monitoring Service and the CORINE land cover datasets for the year 2006. The High-Resolution Layers (HRL) are raster-based datasets, which provide information about different land cover characteristics and are complementary to land-cover mapping (e.g., CORINE 2006) datasets. The soil-related data, field capacity, and saturated hydraulic conductivity were obtained from the High-Resolution Global Map of Soil Hydraulic Properties dataset [39], which provides global maps of the mean values and standard deviations of soil hydraulic parameters based on the Kosugi water retention model in a 1 km resolution for surface soil (0–5 cm). These are estimated from the Kosugi K3 pedotransfer function model (using sand, silt, clay percentages, and bulk density as the inputs) based on the surface soil of the SoilGrids 1 km data set [40]. All these characteristics were interpolated into elevation zones of 200 vertical meters (the first elevation zone starts at 0 m a.s.l. and ends at 200 m a.s.l.). The list of basic characteristics is presented in Table 1.

Table 1. Basic catchment characteristics.

Information	Attribute	Abbrev.	Unit	Min.	Max.	Median
Area	Area	A	km^2	13.7	6214.0	167.3
Elevation	Mean elevation	MELE	m a.s.l.	353	2940	1011
	Mean slope	SL	%	1.7	43.9	18.8
	Elevation range	ER	m	80	3072	1279
	Roughness index	MRI	–	0.15	0.65	0.38
Land use	Forest percentage	FP	%	0.0	94.6	46.9
	Agriculture percentage	AP	%	0.0	92.9	16.3
Climate	Mean annual precipitation	MAP	mm	728	2302	1274
	Mean air temperature	MAT	°C	-2.8	10.3	7.4

Input data for the precipitation and air temperatures from the Spartacus database [41], for the period 2007–2014 were used for the calibration. These data were also interpolated into the hypsometrical elevation zones of 200 vertical meters. Discharge data in the daily time step used for calibration, from the period 2007–2014 were collected from the 209 gauged stations and provided by the Austrian Hydrographic Service. The discharges in all of these catchments are not influenced by dams or hydropower plants. According to the availability of the data, the validation of the model parameters was done for the period 2015–2016 for the runoff and 2015–2018 for the soil moisture. A total of 189 catchments were validated (65 Alpine and 124 Lowland catchments).

The potential evapotranspiration (EP) was estimated with a modified Blaney-Criddle equation [42]:

$$EP = -1.55 + 0.96 \times (8.128 + 0.457 \times T) \times \frac{SD}{Sy} \times 100\ [mm] \quad (1)$$

where:

T—is the mean daily temperature of the catchments (°C),
SD—is the potential duration of sunshine during the day (hours),
Sy—mean annual sum of the potential duration of sunshine (hours),
S_D/S_y—sunshine index (−).

The SD and S_y values were calculated from a digital relief model in GISS GRASS with the r sun function (1 × 1 kmgrid).

The Spartacus climate data were obtained from spatially-distributed climate datasets with a high temporal resolution that extend over several decades [41,43]. The daily precipitation grids have a spacing of 1 km, extend back to 1961, and have been continuously updated. They are constructed according to a classic two-tier analysis involving separate interpolations for the mean monthly precipitation and daily relative anomalies. The former was accomplished by kriging with topographic predictors (external drift kriging) utilizing 1249 stations [43]. The temperature grids were from a gridded dataset of the minimum and maximum daily temperatures covering Austria at a 1 km resolution, which extends back to 1961 as the precipitation dataset.

In [41], an interpolation method was adapted to estimate altitudinal temperature profiles, which also accounts for the spatial representativeness of the station measurements data. In addition, it accounts for the complex and highly variable air temperature distributions in the high mountains. One hundred and fifty station series in Austria and neighboring countries were homogenized (where available) to cover the entire study period and used as the basis of the spatial analysis. Data gaps were also filled.

To improve the soil component reaction of the catchments, the same new experimental data of the Soil Water Index (SWI) were used from the experimental version of the Metop ASCAT Surface Soil Moisture v2 product as in Tong [12]. The original ASCAT surface soil moisture dataset at 12.5 km spatial resolution (before disaggregation to 500 × 500 m) is based on a new parametrization for the correction of vegetation [44], which has shown

better results for Austria [45]. The process of disaggregation consists of a directional resampling method using a connection between regional (12.5 km) and local (0.5 km) scale Sentinel-1 backscatter observations, which retain temporally stable soil moisture patterns that are also reflected in the radar backscatter measurements [1]. This product consists of the surface and root zone soil moisture represented by the Soil Water Index (SWI), which is determined by an exponential filter introduced by [1], and [46,47], with characteristic time delays (T). The T value represents the reduction of the infiltration of the soil moisture dynamics, with higher T values corresponding to a higher degree of reduction. In order that information on short-term conditions is not lost due to soil moisture dynamics still present in the deeper soil layers, T must be carefully chosen. The study [2] compared the ASCAT SWI dataset on in situ soil moisture and found that SWI better agrees with in situ soil moisture from deeper layers than the original set of soil surface moisture data. In addition, the authors they associated the T-value with the soil depth layers and found that the T-values 10 and 20 led to the highest correlations in the shallow subsurface (about 0–20 cm). To avoid losing short-term soil moisture dynamics, a value of T = 10 days was selected in this study. Moreover, for excluding invalid ASCAT measurements affected by snow and frozen soil, the soil moisture is masked by the soil temperature and ECMWF snow cover data from Copernicus Climate Service (ERA5-Land, when soil temperatures at a depth of 0–7 cm are below 1 °C or the snow cover exceeds 30% pixels.

The ASCAT product used in our study contains data for the period 2007–2018 for two soil layers (the surface soil and root zone soil layer). The ASCAT data were interpolated from the 500 × 500 m grid to the same elevation zones as the other input data.

3. Methods

3.1. Conceptual Dual-Layer Hydrological Model

For the rainfall-runoff modelling in the 209 Austrian catchments, the TUW_dual conceptual dual-layer hydrological model as a package in R studio [25], was applied. The TUW hydrological model, which follows the structure of the HBV model, was developed at the Vienna University of Technology by [25], as a lumped or semi-distributed conceptual rainfall-runoff model. It works in a daily or shorter time step and consists of snow, soil moisture, and flow routing routines. The snow submodel represents the processes of the accumulation and melting of the snow in a catchment. The soil moisture submodel represents the processes of the accumulation of water in the soil and evaporation of water from the soil. The flow routing submodel represents the processes of the runoff transformation. Compared to the original TUW model, the TUW_dual hydrological model [25], has a dual representation of the soil layer. The soil submodel is divided into two parts, i.e., the surface soil layer and the root zone soil layer. The soil storage is represented by a thin surface soil layer (dQ_{skin} Figure 2) on the surface and sits on top of the root soil reservoir.

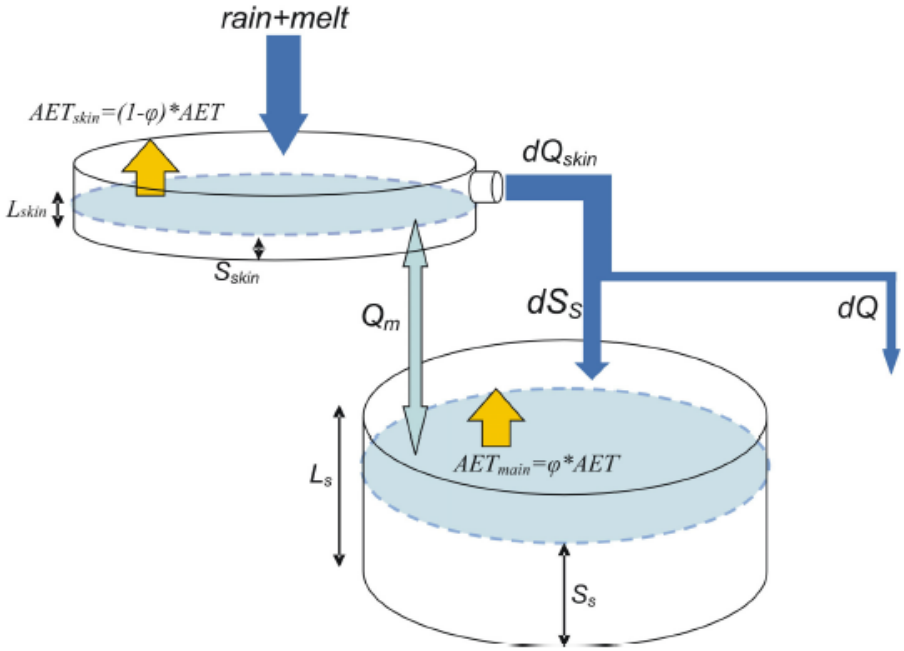

Figure 2. General schematic of the dual-layer soil moisture accounting scheme introduced in the TUW_dual model [25]. Reproduced with permission from [Juraj Parajka], [Matching ERS scatterometer based soil moisture patterns with simulations of a conceptual dual layer hydrologic model over Austria, Hydrol. Earth Syst. Sci., 13, 259–271, 2009]; published by [www.hydrol-earth-syst-sci.net/13/259/2009/, accessed on 24 November 2021].

The surface soil reservoir is fed by rain and melted snow. If the L_{skin} capacity is reached, the dQ_{skin} flow is divided into two parts: (1) dQ becomes the direct runoff, and (2) dS_s increases the root soil moisture Ss. The water in the surface soil moisture reservoir is reduced by a fraction of the actual evaporation, $AET_{skin} = (1 - \varphi)$ AET, where AET is the actual evaporation, and the parameter φ subdivides the AET into evaporation from the AET_{main} root and AET_{skin} surface soil layer. The bidirectional moisture flux Q_m connects the surface and root soil reservoir. Q_m is assumed to be a linear function of the vertical soil moisture gradient Δm:

$$Q_m = \Delta m \times \alpha_m, \quad (2)$$

where α_m is a transfer parameter. If the soil moisture of the surface layer is greater than the soil moisture of the root layer, percolation from the top to the root soil layer ($Q_m > 0$) occurs. If the surface soil moisture is lower than the soil moisture of the root layer, the capillary ascent from the root to the surface layer occurs ($Q_m < 0$). The vertical soil moisture gradient is defined as the difference between the relative soil moisture in the surface soil reservoir and that in the root soil reservoir, i.e.,:

$$\Delta m = \frac{S_{skin}}{L_{skin}} - \frac{S_s}{L_s} \quad (3)$$

where S_{skin} is the surface soil moisture; L_{skin} is the capacity of the surface soil reservoir; and S_s and L_s are the moisture levels and the capacity of the root soil reservoir.

The dual-layer soil moisture accounting scheme uses three parameters for the surface soil layer: the fc_skin-field capacity, i.e., maximum soil moisture storage of the surface skin layer, α-transfer parameter, and φ—parameter for the fraction of the actual evapotranspiration. The root zone soil layer contains the following parameters: Lprat: the limit for potential evaporation, FC: the field water capacity, and BETA: the nonlinear parameter for runoff production. For more information, see, [25]. The list of TUW dual model parameters with their ranges is summarized in Table 2.

Table 2. TUW_dual model parameters with their ranges for 209 Austrian catchments [25]. Reproduced with permission from [Juraj Parajka], [Matching ERS scatterometer based soil moisture patterns with simulations of a conceptual dual layer hydrologic model over Austria, Hydrol. Earth Syst. Sci., 13, 259–271, 2009]; published by [www.hydrol-earth-syst-sci.net/13/259/2009/, accessed on 24 November 2021].

Abbreviation	Description of the Model Parameters	Parameter Range
1. SCF	factor correcting snow measurements	(0.9–1.5 (−))
2. DDF	degree day factor for snowmelt	(0.0–5.0 (mm/°C/day))
3. Tr	temperature threshold, above which precipitation is considered liquid	(1.0–3.0 (°C))
4. Ts	temperature threshold, below which precipitation is considered solid	(−3.0–1.0 (°C))
5. Tm	temperature threshold, above which snowmelt occurs	(−2.0–2.0 (°C))
6. Lprat	parameter limiting potential evaporation	(0.0–1.0 (–))
7. FC	maximum soil moisture storage index, field capacity	(0–600 (mm))
8. BETA	parameter governing runoff generation	(0.0–20.0 (–))
9. k0	storage coefficient governing very fast runoff response	(0.0–2.0 (days))
10. k1	storage coefficient governing fast runoff response	(2.0–30.0 (days))
11. k2	storage coefficient governing slow runoff response	(30.0–250 (days))
12. lsuz	threshold parameter storage state for initiation of the very fast runoff response	(1.0–100 (mm))
13. cperc	constant percolation rate	(0.0–8.0 (mm/day))
14. bmax	maximum base at low flows	(0.0–30.0 (days))
15. croute	free scaling parameter for routing	(0.0–50.0 ($days^2$ /mm)
16. fc_skin	field capacity, i.e., maximum soil moisture storage of the surface layer	(0.1–10 (mm))
17. α	non-linearity coefficient of runoff generation	(0.7–0.95 (−))
18. ϕ	parameter for the fraction of the actual evaporation	(5–15 (−))

3.2. Calibration

For the calibration and multi-objective calibration parameters of the TUW_dual model, the Differential Evolution algorithm (DEoptim) [48], was applied. The TUW_dual model was calibrated to 4 different objective functions (OF): OF_Q based on runoff Q, OF_{Q+SR} based on the runoff and soil moisture in the root layer, OF_{Q+SS} based on the runoff and soil moisture in the surface layer, and $OF_{Q+SR+SS}$ based on the runoff and soil moisture both in the root and surface layers.

The individual objective functions of OF_Q for the runoff, OF_{SR} for the soil moisture in the root layer, and OF_{SS} for the soil moisture in the surface layer were calculated using a combination of the Nash-Sutcliffe efficiency coefficient NSE (Nash and Sutcliffe) [49], and the logarithmic NSE, where OF = (NSE + LogNSE)/2. In the objective functions OF the simulated values of the runoff Q_{sim}, soil moisture in the surface layer SM_{sim} (surface) and in the root soil layer SM_{sim} (root) were compared with the measured runoff Q_{obs} and the measured soil moisture SWI_{root} and $SWI_{surface}$ from the ASCAT data.

Different weights for the individual objective functions OF_Q, OF_{SR}, and OF_{SS} were set in the multi-objective functions:

$$OF_{Q+SR} = OF_Q \times w_Q + OF_{SR} \times w_{SR}, \quad (4)$$

$$OF_{Q+SS} = OF_Q \times w_Q + OF_{SS} \times w_{SS}, \quad (5)$$

$$OF_{Q+SR+SS} = OF_Q \times w_Q + OF_{SR} \times w_{SR} + OF_{SS} \times w_{SS}, \quad (6)$$

where w_Q, w_{SR} and w_{SS} are the weights. In OF_{Q+SR} and OF_{Q+SS}, the values of the weights w_Q, w_{SR} and w_{SS} are 1/2, and in $OF_{Q+SR+SS}$, the values of the weights w_Q, w_{SR} and w_{SS} are 1/3, [12,50]. This choice is based on Tong's [12] paper, where it was also detected that the calibration weight for runoff > 0.3 provides solid calibration results of (RME > 0.7).

For the estimation of the runoff model efficiency (RME), we used a combination of the Nash–Sutcliffe efficiency coefficient (NSE) and the logarithmic NSE:

$$RME = \frac{(NSE + logNSE)}{2}, \quad (7)$$

$$\mathrm{NSE} = 1 - \frac{\Sigma_{i=1}^{n}\left(Q_{obs} - Q_{simi}\right)^2}{\Sigma_{i=1}^{n}\left(Q_{obsi} - \overline{Q}_{obs}\right)^2}, \quad (8)$$

$$\mathrm{logNSE} = 1 - \frac{\Sigma_{i=1}^{n}\left(\log Q_{obs} - \log Q_{simi}\right)^2}{\Sigma_{i=1}^{n}\left(\log Q_{obsi} - \log \overline{Q}_{obs}\right)^2}, \quad (9)$$

where Q_{sim}, Q_{obs} are the simulated and observed runoff; $\overline{Q}_{obs}$ is the average of the observed flow.

The volume error (VE) of the runoff estimation was calculated by:

$$\mathrm{VE} = \frac{\sum_{i=1}^{n} Q_{sim}^{i} - \sum_{i=1}^{n} Q_{obs}^{i}}{\sum_{i=n}^{n} Q_{obs}^{i}} \quad (10)$$

The efficiency of the model to simulate soil moisture was assessed by the correlation between the relative values of the simulated soil moisture for the root and top zones $SM_{sim(root)}$ and $SM_{sim(surface)}$ and the measured values of the SWI_{root} and $SWI_{surface}$ soil moisture from the ASCAT data:

$$\mathrm{Correlation}\left(\mathrm{R\,SWI}_{root}\right) = \left(\frac{SM_{sim\ (root)}}{FC} \times 100\right) \text{ and } SWI_{root}, \quad (11)$$

$$\mathrm{Correlation}\left(\mathrm{R\,SWI}_{surface}\right) = \left(\frac{SM_{sim\ (surface)}}{fc_{surface}} \times 100\right) \text{ and } SWI_{surface}, \quad (12)$$

4. Results

4.1. Calibration

Firstly, we calibrated the TUW dual model for the 209 Austrian catchments in the period 2007–2014 only to runoff Q. Secondly, the multi-objective calibration was run for the three versions of the objective function: OF_{Q+SR}, OF_{Q+SS}, and $OF_{Q+SR+SS}$. With the best sets of the model parameters, the daily values of the soil moisture in both the surface and root soil layers were simulated for each individual catchment and the period 2007–2014.

The cumulative distribution functions (CDFs) of the values of the runoff model efficiency (RME), runoff volume error (VE), and correlation coefficient R between the simulated (SM_{sim}) and measured (SWI) soil moisture in the root and surface layers for the two groups of catchments (71 Alpine and 138 Lowland catchments) are compared in Figure 3. The medians of the values of the runoff model efficiency, runoff volume error, and correlation coefficients are summarized in Table 3.

Table 3. Medians of the runoff model efficiency values, runoff volume error, and correlation coefficients between simulated and measured surface and root soil moisture for the two groups of catchments (71 Alpine and 138 Lowland catchments) in the calibration period 2007–2014.

Calibration Variant (2007–2014)	RME		VE (-)		R Surface Soil Moisture		R Root Soil Moisture	
	Alpine	Lowland	Alpine	Lowland	Alpine	Lowland	Alpine	Lowland
Cal. to Q	0.83	0.75	−0.05	0.02	0.02	0.37	0.23	0.49
Cal. to Q + SS	0.81	0.74	−0.05	0.02	0.40	0.49	0.36	0.49
Cal. to Q + SR	0.81	0.74	−0.05	0.02	0.18	0.38	0.43	0.54
Ca. to Q + SS + SR	0.81	0.73	−0.04	0.03	0.41	0.48	0.44	0.54

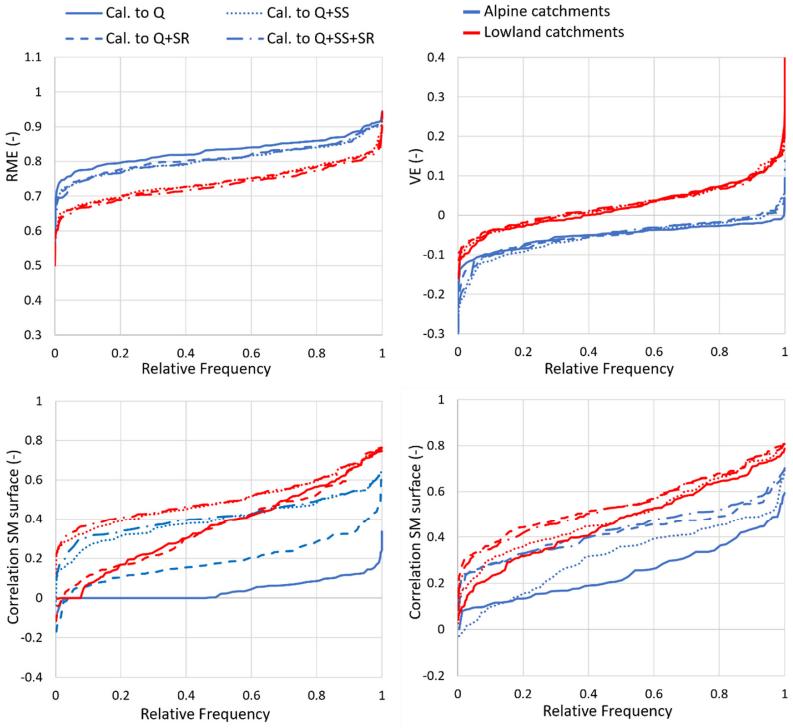

Figure 3. Cumulative distribution functions (CDFs) of the values of the runoff model efficiency (top left), runoff volume error (top right), and correlation coefficients between the simulated and measured surface soil moisture (bottom left) and root soil moisture (bottom right) in the calibration period 2007–2014. CDFs are plotted for the four calibration variants. The red and blue lines show the calibration variants for the group of 138 Lowland (red) and 71 Alpine catchments (blue), respectively.

From the CDFs in Figure 3, it can be seen that in all the cases of the calibration variants, the values of RME are higher for the Alpine than for the Lowland catchments. The calibration for the soil moisture (Cal to Q + SS, Cal to Q + SR, and Cal to Q + SS + SR) also slightly decreases the values of RME both in the Alpine and Lowland catchments. These results are confirmed in Table 3, where the median of RME varies from 0.83 to 0.81 in the Alpine catchments and from 0.75 to 0.73 in the Lowland catchments.

In the Alpine catchments, an underestimation of the simulated volumes of the runoff is visible; the median of the values of VE in Table 3. varies from −0.05 to −0.04. These results could be caused by an underestimation of the snow precipitation in the Alpine catchments, but generally, the VE values are relatively low. In the Lowland catchments, the simulated volumes of the runoff are slightly overestimated; the median of the VE values varies from 0.02 to 0.03.

From the CDFs of the correlation coefficients between the simulated and measured soil moisture both in the surface and root soil layers, it is evident that in the case of the calibration only for the runoff, the values of the correlation coefficients are very low in the Alpine catchments. The median of the values of the correlation coefficients for the surface soil layer is only 0.02 and 0.23 for the root soil layer. The calibration for the soil moisture improved the results in the case of the calibration both for the runoff, surface, and root soil moisture (Cal to Q + SS + SR); the median of the correlation coefficients increased to 0.41 for the surface soil layer and to 0.44 for the root soil layer. In the Lowland catchments, the values of the correlation coefficients between the simulated and measured soil moisture are much higher. In the case of the calibration only for the runoff, the median of the correlation coefficients is 0.37 for the surface soil layer and 0.49 for the root soil layer. In the case of the calibration for the runoff and both the surface and root soil moisture (Cal to Q + SS + SR), the median of the values of the correlation coefficients increased to 0.48 for the surface and 0.54 for the root soil layer.

4.2. Validation of the Model Efficiency

4.2.1. Validation of the Runoff Model Efficiency for the Period 2015–2016

In the validation of the runoff for 2015–2016, we validated the model parameters from the calibration period and four variants of the objective functions. The cumulative distribution functions of the values of the runoff model efficiency (RME) and volume error (VE) are compared in Figure 4. The medians of the values of RME, VE, and correlation coefficients between the simulated and measured soil moisture of the surface and root soil layers are introduced in Table 4.

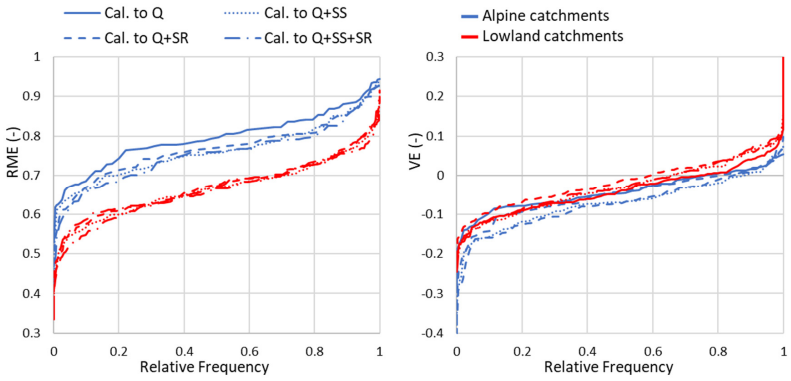

Figure 4. Cumulative distribution functions (CDFs) of the values of the runoff model efficiency (surface left) and runoff volume error (surface right) in the validation period 2015–2016. The CDFs were plotted for four calibration variants of the objective functions. The red and blue lines show the calibration variants for the group of 124 Lowland (red) and 65 Alpine catchments (blue), respectively.

Table 4. Medians of the values of the runoff model efficiency (RME) and runoff volume error (VE) for the four calibration variants and two groups of catchments (65 Alpine and 124 Lowland) in the validation period 2015–2016.

Calibration Variant	RME (−)		VE (−)	
	Alpine	Lowland	Alpine	Lowland
Runoff (Q)	0.80	0.67	−0.05	−0.04
Q + SS	0.76	0.67	−0.07	−0.03
Q + SR	0.77	0.68	−0.04	−0.01
Q + SS + SR	0.76	0.67	−0.07	−0.03

The validation results confirmed the sufficient efficiency of the model with the calibrated parameters to simulate runoff in the validation period. Again, the values of RME are better for the Alpine than for the Lowland catchments. Similarly, as in the calibration period, the parameters calibrated for the soil moisture (Cal to Q + SS, Cal to Q + SR, and Cal to Q + SS + SR) slightly decreased the values of RME in the Alpine catchment and did not change the results of RME in the Lowland catchments. The medians of the values of RME for the Alpine catchments are a little lower than in the calibration period and vary from 0.80 to 0.76. For the Lowland catchments, the medians of RMEs have a value of 0.67. The medians of the values of the volume error vary from −0.05 to −0.07 in the Alpine catchments and from −0.04 to −0.01 in the Lowland catchments. Although in both the Alpine and the Lowland catchments, the volume of runoff was slightly underestimated, in the case of the Lowland catchments, the parameters calibrated also for the soil moisture slightly decrease the volume errors.

4.2.2. Validation of the Soil Moisture for the Period 2015–2018

In the validation for the period 2015–2018, we validated the model parameters only for the soil moisture due to the fact that we did not have measured runoff data available

for the period 2017–2018. Therefore, we compared the correlation coefficients between the simulated (SM_{sim}) and measured ASCAT (SWI) soil moisture values, Figure 5.

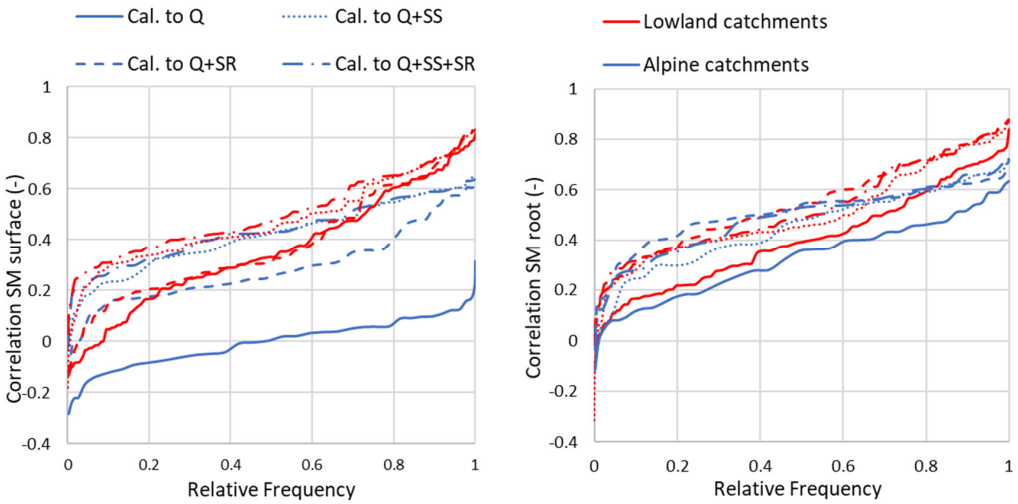

Figure 5. Cumulative distribution functions (CDFs) of the correlation coefficients of surface soil moisture (bottom left) and of the root zone soil moisture (bottom right) in the validation period 2015–2018. The CDFs are plotted for the four calibration variants. The red and blue lines show the calibration variants for the group of 124 Lowland (red) and 65 Alpine catchments (blue), respectively.

When comparing the correlation coefficients between the simulated and measured soil moisture, we again detected better results in the Lowland than in the Alpine catchments and an improvement using the model parameters from a multi-objective calibration. In the surface soil layer, the median of the correlation coefficients increased from 0.01 (calibration only for the runoff) to 0.43 (the calibration to runoff, surface and root soil moisture) in the Alpine catchment and from 0.33 (calibration only for the runoff) to 0.48 (the calibration for the runoff, surface and root soil moisture) in the Lowland catchments. In the root soil layer, the median of the correlation coefficients increased from 0.36 (calibration only for the runoff) to 0.53 (the calibration for the runoff, surface and root soil moisture) in the Alpine catchments and from 0.40 (calibration only for the runoff) to 0.49 (the calibration for the runoff, surface, and root soil moisture) in the Lowland catchments, see Table 5.

Table 5. Medians of the correlation coefficients of the surface and root soil moisture for the two groups of catchments (65 Alpine and 124 Lowland catchments) in the validation period 2015–2018.

Calibration Variant	Median of R of Surface Soil Moisture		Median of R of Root Soil Moisture	
	Alpine	Lowland	Alpine	Lowland
Runoff (Q)	0.01	0.33	0.36	0.40
Q + SS	0.43	0.46	0.48	0.46
Q + SR	0.27	0.33	0.54	0.54
Q + SS + SR	0.43	0.48	0.53	0.49

4.3. Improvement of the Model Efficiency

4.3.1. Improvement in the Calibration

In our comparison of the correlation coefficients R between the simulated and measured soil moisture, which were separate for the root zone and surface zone, we detected that the calibration for the soil moisture increased the values of R. The improvement mostly depended on which measured ASCAT soil moisture values (root or surface) were used in the calibration process and subsequently in the correlations. From the results documented in Table 6, it is seen that for the variants of the multi-objective calibration for the runoff and both surface and root soil moistures 71 (100%) of the Alpine and 137 (99%) of the Lowland

catchments improved in the correlation coefficients between the simulated and measured surface soil moisture, and 68 (96%) of the Alpine and 130 (94%) of the Lowland catchments improved in the correlation coefficients between the simulated and measured root soil moisture. In general, almost all of the catchments have shown improved calibration results.

Table 6. The number of improved catchments in the correlations of the surface soil (SS) and root soil (SR) moisture, in 209 catchments in the calibration period 2007–2014.

Number of Improved Catchments R SS	**Alpine (71)**		**Lowland (138)**	
	(Num.)	**(%)**	**(Num.)**	**(%)**
Q + SS	69	97	138	100
Q + SR	56	79	73	53
Q + SR + SS	71	100	137	99
Number of Improved Catchments R SR	**Alpine (71)**		**Lowland (138)**	
	(Num.)	**(%)**	**(Num.)**	**(%)**
Q + SS	39	55	87	63
Q + SR	71	100	136	99
Q + SR + SS	68	96	130	94

4.3.2. Improvement in the Validation

Comparing the values of RME from the validation of the runoff and period 2015–2016, we detected that the parameters of the model calibrated both for the runoff and soil moisture did not improve the medians of the values of RME either in the Alpine or the Lowland catchments. However, improvement in the individual values of RMEs was indicated in some Lowland catchments, where the RMEs increased in 49 (40%) catchments for the calibration variant Q + SS, in 62 (50%) catchments for the calibration variant Q + SR, and in 47 (38%) catchments for the calibration variant Q + SS + SR (Table 7).

Table 7. The number/percentage of improved Alpine and Lowland catchments in the RMEs in the validation period 2015–2016.

Runoff Model Efficiency (RME) 189 Catchments 2015–2016	**Number of Improved Catchments RME**	**Alpine (65)**		**Lowland (124)**	
	(Num.)	**(Num.)**	**(%)**	**(Num.)**	**(%)**
Q + SS	56	7	11	49	40
Q + SR	68	6	9	62	50
Q + SS + SR	51	4	6	47	38

When comparing the correlation coefficients R, we detected that similar to the calibration, the categorization between the Alpine and Lowland groups of catchments did not play as important a role as expected. The improvement depends on which soil layer (surface or root) is used for the validation (see Table 7).

The improvement in correlation between the simulated and measured soil moisture was detected for the majority of both groups of catchments. For the variants of the parameter calibrated for the runoff and both surface and root soil moisture, the improvement in R for the surface soil moisture was in 63 (97%) Alpine and in 110 (89%) Lowland catchments, and the improvement in R for root soil moisture was in 54 (83%) Alpine and in 110 (89%) Lowland catchments, Table 8 and Figure 6.

Table 8. Correlation coefficients between the simulated and measured soil moisture in the surface and root soil layers for 189 catchments in the validation period 2015–2018, and comparison of the number of improved Alpine (65) and Lowland (124) catchments in the correlation coefficients.

Number of Improved Catchments R SS	**Alpine (65)**		**Lowland (124)**	
	(Num.)	**(%)**	**(Num.)**	**(%)**
Q + SS	58	89	99	80
Q + SR	56	86	83	67
Q + SS + SR	63	97	110	89
Number of Improved Catchments R SR	**Alpine (65)**		**Lowland (124)**	
	(Num.)	**(%)**	**(Num.)**	**(%)**
Q + SS	45	69	98	79
Q + SR	57	88	110	89
Q + SS + SR	54	83	110	89

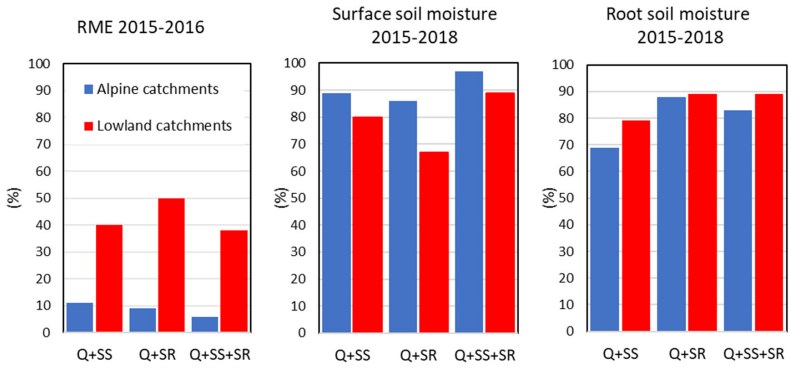

Figure 6. Percentage of Alpine and Lowland catchments for which Q + SS, Q + SR and Q + SS + SR led to improvement compared to Q, between the simulated and measured surface and root soil moisture in the validation periods 2015–2016 and 2015–2018, respectively the (blue) Alpine catchments and (red) Lowland catchments.

In addition, we evaluated the improvement in the values of RME, R SS and R SR in the validation period, concerning selected catchment topographical and land use characteristics: MELE- mean elevation (m a.s.l.), SL- the slope of the terrain (%), FP—the percentage of the forest coverage (%), and AP- the percentage of the agricultural lands (%). The description of these characteristics is in Table 1 in Chapter 2. Based on this evaluation, all catchments were divided into classes where the assimilation of the SWI improved the values of RME, RR SS and R SR (the classes are marked with (+)), and the classes where these values were not improved (the classes are marked with (−)). For each class of the catchments, the number and percentage of the catchments and the medians of the selected catchment characteristics (MELE, SL, FP and AP) are shown in Table 9.

From the results in Table 9, it is seen that the assimilation of the SWI in the model calibration improved the RMEs in the catchments with a lower mean catchment elevation (the median of MELE ranges from 738.5 to 754.9 m a.s.l), a lower mean slope of the terrain (the median of SL ranges from 10.44 to 12.43%), and with a higher percentage of agricultural land (the median of AP ranges from 26.8 to 38.1%). In the contrary, the improvements were not indicated in the catchments with a higher mean catchment elevation (the median of MELE ranges from 1270.9 to 1335.4 m a.s.l), a higher mean slope of the terrain (the median of SL ranges from 23.61 to 24.73%) and a lower percentage of agricultural land (the median of AP ranges from 10.9 to 11.4%). An improvement in the values of RME only slightly depends on the percentage of forest coverage. The percentage of forest cover and the percentage of agricultural land plays an essential role in the improvement of the soil moisture simulations. The values of R SR were improved in the catchments with a lower mean slope of the terrain (the median of SL ranges from 16.06 to 18.54%), a lower

percentage of forest coverage (the median of FP ranges from 45.3 to 46.3%) and with a higher percentage of agricultural land (the median of FP ranges from 18.2 to 20.1%). The improvement of R SR was not indicated in the catchment with a higher mean slope of the terrain (the median of SL ranges from 23.4 to 24.7%), a higher percentage of forest coverage (the median of FP ranges from 63.1 to 78.4%) and with a lower percentage of agricultural land (the median of FP ranges from 5.9 to 8.0%). The similar results we also indicated in the improvements in the values of R SS.

Table 9. The medians of the catchment characteristics where the values of RME, R SS and RSR were improved (+) and were not improved (−).

Discharge Simulation for the Period 2015–2016							
RME	**[Num.]**	**[%]**	**Imp./Not Imp.**	**MELE**	**SL**	**FP**	**AP**
Q + SS	56	30	(+)	754.9	12.43	53.8	26.8
Q + SR	68	36	(+)	738.5	10.44	45.5	31.2
Q + SS + SR	51	27	(+)	744.5	10.83	50.9	38.1
Q + SS	133	70	(−)	1270.9	23.61	46.3	11.4
Q + SR	121	64	(−)	1335.4	24.73	46.9	10.9
Q + SS + SR	138	73	(−)	1279.4	23.84	46.4	11.3
Soil moisture correlation for period 2015–2018							
R SS	[Num.]	[%]	imp./not imp.	MELE	SL	FP	AP
Q + SS	144	76	(+)	1076.9	19.36	45.5	16.3
Q + SR	135	71	(+)	1192.9	21.83	46.3	15.3
Q + SS + SR	166	88	(+)	1101.9	20.20	46.5	15.7
Q + SS	45	24	(−)	1020.7	19.73	67.6	9.1
Q + SR	54	29	(−)	892.0	17.04	52.8	16.3
Q + SS + SR	23	12	(−)	941.1	18.54	78.6	9.1
Soil moisture correlation for period 2015–2018							
R SR	[Num.]	[%]	imp./not imp.	MELE	SL	FP	AP
Q + SS	137	73	(+)	940.2	16.06	45.3	20.1
Q + SR	159	84	(+)	1067.3	18.54	46.3	18.2
Q + SS + SR	160	85	(+)	1006.9	17.95	46.3	18.5
Q + SS	52	27	(−)	1204.5	24.67	63.1	8.0
Q + SR	30	16	(−)	1016.5	23.38	78.4	5.9
Q + SS + SR	52	27	(−)	1105.4	23.49	64.7	7.3

1 ↑ lower value
2
3 average
4
5
6 ↓ higher value

5. Discussion

By testing the quality of the ASCAT data, we detected the missing data in the winter months (probably due to the snow cover), which is typical of this type of data as seen in other works [10,51]. However, from the spring to the autumn months, the ASCAT data coverage was stable without any missing or error data.

The results of the calibration for the four calibration variants (for the runoff, the runoff and surface soil moisture, the runoff and root soil moisture, and the runoff and both surface and root soil moisture) confirmed that the efficiency of the model to simulate runoff is higher in the Alpine than in the Lowland catchments. These results may be due to the semi-distributed structure of the TUW_dual model, which allows for the better simulation of the runoff in the catchments with higher altitudinal zonality and higher dynamics of surface and subsurface flows than in the Lowland catchments. The same findings were obtained in [51]. The calibration for the soil moisture also slightly decreased the RMEs in both groups of catchments. As for the volume error values, in the Alpine catchments, an underestimation of the simulated volumes of the runoff is visible; the median of VE values varied from −0.05 to −0.04. These results could be caused by an underestimation of the snow precipitation in the Alpine catchments or by processes of melting glaciers that are not considered in the model structure. In the Lowland catchments, the volume of runoff was slightly overestimated; the median of VE values varied from 0.02 to 0.03. Generally, the VE values in both groups of the catchments were relatively low.

The efficiency of the model to simulate soil moisture with the parameters calibrated only for the runoff was very low in the Alpine catchments. However, the combined use of soil moisture and runoff in the calibration improved the soil moisture simulation in the majority of the catchments, except for the catchments with higher forest cover percentages, where the reason for the lower quality of satellite soil moisture products is dense vegetation. The limitation of the quality of satellite soil moisture products in forested areas is mentioned in [20,52].

When compared to the Alpine catchments, a more significant improvement of the hydrological model efficiency to simulate soil moisture was achieved in the lowlands, which can be related to the higher quality of the ASCAT soil moisture retrievals in contrast to the high mountains. This can also be related to the lower spatial variability in the soil texture and land cover categories, the milder slopes, and moderate variations in the elevations (see Table 9).

The results of the validation confirmed the sufficient efficiency of the model with calibrated parameters to simulate runoff and soil moisture in the validation periods. In the validation of the runoff, the RME values are again better for the Alpine than for the Lowland catchments. Similarly, as in the calibration period, the calibration for the soil moisture slightly decreases the values of RME in the Alpine catchments. In the Lowland catchments, the calibration for the soil moisture did not change the results of the RME. The validation of the soil moisture again confirmed better results in the Lowland than in the Alpine catchments and improved soil moisture simulations using the model parameters from the multi-objective calibration (in comparison with the calibration only for the runoff) in both groups of the catchments.

In general, with the assimilation of the scatterometer soil moisture, we detected a considerable improvement in the soil moisture simulation versus the measured SWI as in [11,12,16,20,25]. The findings of this paper are consistent with the paper by [12,25]. In Tong et al. [12] the same type of the ASCAT soil moisture data was used, however, only SWI for the root zone was implemented. In that paper, the ASCAT product of the SWI root was applied for the calibration of the TUW model with 15 parameters for the same 209 Austrian catchments as in our paper. In Tong's [12] paper, with different calibration weights in the objective functions for the runoff it was detected that the calibration weight for runoff >0.3 provide stable calibration results (RME > 0.7). This is in accordance with our study where we applied the weight 0.33 for runoff with sufficient results of the RME We also compared the improved catchments from Tong's simulations (Q + SR) and improved catchments from our simulations (Q + SS, Q + SR, Q + SR + SS). In comparing the RMEs and correlation coefficients of the soil moisture, we detected that the improvement was in the same type of catchments, i.e., the catchments with a lower mean elevation and a higher percentage of agricultural land. When we compared the amounts of the improved catchments in RMEs for the same weights of the runoff and SWI in the objective functions, we detected approximately the same amounts of improved catchments. The novelty of our paper in comparison to [12] is using both surface and root zone soil moisture S1-ASCAT data that led to better soil moisture simulations.

In Parajka et al. [25], surface soil moisture observations by an ERS scatterometer with simulations of a conceptual hydrological model with two soils moisture levels (dual-layer model) were compared for 148 Austrian catchments in the period 1991–2000. Higher-level soil moisture values observed by the scatterometer were generally lower than those simulated by the model. The combined use of the ERS scatterometer-based soil moisture and measured runoff in the calibrations delivered more robust model parameter estimates than using either of these two datasets. In the comparison with this study where the spatial resolution of the ASCAT soil moisture data was 12.5 km grid, we applied the higher spatial resolution data of 500 m grid which led to better results of the soil moisture simulations.

The results of our study are also consistent with the studies where the satellite soil moisture data were incorporated in different modelling approaches. The added value of using soil moisture from remote sensing in the calibration of large-scale hydrological

models was addressed in [26]. Improvement of the simulation of runoff discharges in upstream areas was reported. In addition, the remotely-sensed soil moisture resulted in an improved simulation of the moisture content of the soil throughout the catchments. The study's conclusions stressed the potential of including soil moisture data in the calibration of hydrological models.

Improvement of hydrological predictability and reduction of equifinality of the Soil and Water Assessment Tool (SWAT) was evaluated in [27] by testing the relative potential of using estimates of spatially-distributed surface and root zone soil moisture in the calibration. Improvement of soil moisture simulation of the surface soil layer was achieved. However, the soil moisture content in the lower soil layer (and other water balance components such as streamflow and evapotranspiration) was less affected.

The SWAT model was also used in [28]; where raw remotely-sensed surface soil moisture data were used (the soil moisture values were not transformed into a soil water index). The results showed that the approach generally improved the simulation of the rainfall-runoff response concerning delays but could not correct the overall routing behavior. In [29], the efficiency of two calibration schemes (multi-objective and discharge only) for a lumped model and a semi-distributed model with only one and several gauges available for calibration were compared. The same findings, as in our study, were that the multi-objective scheme slightly degraded the streamflow predictions at the gauged sites compared with the streamflow-only calibration; however, improvements occurred in the validation period. Improvement was achieved at the gauged sites not used in the calibration when the remotely-sensed soil moisture data was used.

6. Conclusions

For testing the potential of new satellite datasets of soil moisture (ASCAT) for the multi-objective calibrations of the dual-layer, the TUW_dual conceptual semi-distributed hydrological model was calibrated in 209 Austrian catchments (71 Alpine and 138 Lowland catchments) and validated in 189 catchments (65 Alpine and 124 Lowland catchments) situated in different physiographic and climate zones of Austria. Both the surface soil moisture and root zone soil moisture indexes based on ASCAT data were implemented into the hydrological model calibration and validation.

The calibration and multi-calibration of the TUW_dual model were undertaken in the period 2007–2014. The validation of the model for the runoff was provided in the period 2015–2016 and the validation for the soil moisture in the period 2015–2018.

In general, we can conclude that the assimilation of the new ASCAT product to the objective function of the multi-objective calibration significantly improved the model performance in both the calibration and validation periods, especially in the Lowland catchments (catchments where the rain is a major contributor to the runoff and water from melted snow does not dramatically affect the runoff), except for the catchments with higher forest cover percentages. Improvements were also detect in the runoff model efficiency in the validation period in the Lowland catchments with lower mean elevations, lower terrain slopes, and a higher percentage of agricultural land (compared to the Alpine catchments). What was new compared to similar papers was that we also detected an improved runoff model efficiency and categorized the catchments where the improvement can be expected.

The enhanced model efficiency has important implications for water resource management purposes. The findings strengthen recommendations that hydrological models should consider information beyond runoff signatures in their calibration.

Author Contributions: Conceptualization, M.K., J.P., J.S., K.H. and S.K.; methodology, M.K., J.P., J.S., K.H. and S.K.; software, M.K. and J.P.; validation, M.K. and J.P.; formal analysis, M.K., J.P., J.S., K.H., S.K. and B.A.; investigation, M.K., J.P., J.S., K.H., S.K. and B.A.; resources, M.K., J.P., J.S., K.H., S.K. and R.T.; data curation, J.P., I.P., M.V., R.T. and P.S.; writing, M.K., J.P., J.S., K.H. and S.K.; writing—review and editing, M.K., J.P., J.S., K.H. and S.K.; visualization, M.K., J.P., J.S., K.H. and S.K.; project administration, M.K., J.P., J.S., K.H. and S.K.; funding acquisition, J.P., J.S., K.H. and S.K. All authors have read and agreed to the published version of the manuscript.

Funding: This work was supported by the Slovak Research and Development Agency under Contract No. APVV-18-0347, No. APVV-19-034 and the VEGA Grant Agency No. 1/0632/19. This work has been supported in the frame of the AlpCarp Project No. 2019-10-15-002 under the bilateral program "Action Austria—Slovakia, Cooperation in Science and Education".

Institutional Review Board Statement: Not applicable.

Informed Consent Statement: Not applicable.

Data Availability Statement: The data presented in this study are partly available on request from the corresponding author. Some of the data are only available from the Department of Geodesy and Geoinformation, TU Wien, 1040 Vienna, Austria on a noncommercial basis.

Acknowledgments: This work was supported by the Slovak Research and Development Agency under Contract No. APVV-18-0347, No. APVV-19-034 and the VEGA Grant Agency No. 1/0632/19. At the same time, we would like to acknowledge the support from the Stefan Schwarz grant of the Slovak Academy of Sciences. This work has been supported in the frame of the AlpCarp Project No. 2019-10-15-002 under the bilateral program "Action Austria—Slovakia, Cooperation in Science and Education". The authors thank the agencies for its research support. This work was also supported by the Austrian Science Funds (FWF) as part of the Vienna Doctoral Program on Water Resource Systems (DK W1219-N28), the Austrian Research Promotion Agency (FFG) through the BMon project (Contract No. 866031) in the acknowledgments.

Conflicts of Interest: The authors declare no conflict of interest.

References

1. Wagner, W.; Bloschl, G.; Pampaloni, P.; Calvet, J.-C.; Bizzarri, B.; Wigneron, J.-P.; Kerr, Y. Operational readiness of microwave remote sensing of soil moisture for hydrologic applications. *Hydrol. Res.* **2007**, *38*, 1–20. [CrossRef]
2. Paulik, C.; Dorigo, W.; Wagner, W.; Kidd, R. Validation of the ASCAT soil water index using in situ data from the international soil moisture network. *Int. J. Appl. Earth Obs. Geoinf.* **2014**, *30*, 1–8. [CrossRef]
3. Fang, B.; Lakshmi, V. Soil moisture at watershed scale: Remote sensing techniques. *J. Hydrol.* **2014**, *516*, 258–272. [CrossRef]
4. Muñoz-Sabater, J.; Al Bitar, A.; Brocca, L. Soil moisture retrievals based on active and passive microwave data: State-of-the-art and operational applications. In *Satellite Soil Moisture Retrievals: Techniques and Applications*; Petropoulos, G.P., Srivastava, P., Kerr, Y., Eds.; Elsevier: Amsterdam, The Netherlands, 2016; Volume 18, pp. 351–378.
5. Kim, H.; Parinussa, R.; Konings, A.; Wagner, W.; Cosh, M.H.; Lakshmi, V.; Zohaib, M.; Choi, M. Global-scale assessment and combination of SMAP with ASCAT (active) and AMSR2 (passive) soil moisture products. *Remote Sens. Environ.* **2018**, *204*, 260–275. [CrossRef]
6. Beck, H.E.; Pan, M.; Miralles, D.G.; Reichle, R.H.; Dorigo, W.A.; Hahn, S.; Sheffield, J.; Karthikeyan, L.; Balsamo, G.; Parinussa, R.M.; et al. Evaluation of 18 satellite-and model-based soil moisture products using in situ measurements from 826 sensors. *Hydrol. Earth Syst. Sci.* **2021**, *25*, 17–40. [CrossRef]
7. Wagner, W.; Hahn, S.; Kidd, R.; Melzer, T.; Bartalis, Z.; Hasenauer, S.; Figa-Saldaña, J.; De Rosnay, P.; Jann, A.; Schneider, S.; et al. The ASCAT soil moisture product: A review of its specifications, validation results, and emerging applications. *Meteorol. Z.* **2013**, *22*, 5–33. [CrossRef]
8. Moran, M.S.; Doorn, B.; Escobar, V.; Brown, M.E. Connecting NASA science and engineering with earth science applications. *J. Hydrometeorol.* **2015**, *16*, 473–483. [CrossRef]
9. Tebbs, E.; Gerard, F.; Petrie, A.; De Witte, E. Emerging and potential future applications of satellite-based soil moisture products. In *Satellite Soil Moisture Retrievals: Techniques and Applications*; Petropoulos, G.P., Srivastava, P., Kerr, Y., Eds.; Elsevier: Amsterdam, The Netherlands, 2016; Volume 19, pp. 379–400.
10. Brocca, L.; Crow, W.T.; Ciabatta, L.; Massari, C.; de Rosnay, P.; Enenkel, M.; Hahn, S.; Amarnath, G.; Camici, S.; Tarpanelli, A.; et al. A review of the applications of ASCAT soil moisture products. *IEEE J. Sel. Top. Appl. Earth Obs. Remote Sens.* **2017**, *10*, 2285–2306. [CrossRef]
11. Brocca, L.; Ciabatta, L.; Massari, C.; Camici, S.; Tarpanelli, A. Soil Moisture for Hydrological Applications: Open Questions and New Opportunities. *Water* **2017**, *9*, 140. [CrossRef]
12. Tong, R.; Parajka, J.; Salentinig, A.; Pfeil, I.; Komma, J.; Széles, B.; Kubáň, M.; Valent, P.; Vreugdenhil, M.; Wagner, W.; et al. The value of ASCAT soil moisture and MODIS snow cover data for calibrating a conceptual hydrologic model. *Hydrol. Earth Syst. Sci.* **2021**, *25*, 1389–1410. [CrossRef]
13. Naeimi, V.; Scipal, K.; Bartalis, Z.; Hasenauer, S.; Wagner, W. An improved soil moisture retrieval algorithm for ERS and METOP scatterometer observations. *IEEE Trans. Geosci. Remote Sens.* **2009**, *47*, 1999–2013. [CrossRef]
14. Steele-Dunne, S.; Hahn, S.; Wagner, W.; Vreugdenhil, M. Towards including dynamic vegetation parameters in the EUMETSAT H SAF ASCAT soil moisture products. *Remote Sens.* **2021**, *13*, 1463. [CrossRef]

15. Brocca, L.; Melone, F.; Moramarco, T.; Morbidelli, R. Antecedent wetness conditions based on ERS scatterometer data. *J. Hydrol.* **2009**, *364*, 73–87. [CrossRef]
16. Tramblay, Y.; Bouaicha, R.; Brocca, L.; Dorigo, W.; Bouvier, C.; Camici, S.; Servat, E. Estimation of antecedent wetness conditions for flood modelling in northern Morocco. *Hydrol. Earth Syst. Sci.* **2012**, *16*, 4375–4386. [CrossRef]
17. Sunwoo, W.; Choi, M. Robust initial wetness condition framework of an event-based rainfall–runoff model using remotely sensed soil moisture. *Water* **2017**, *9*, 77. [CrossRef]
18. Jadidoleslam, N.; Mantilla, R.; Krajewski, W.; Goska, R. Investigating the role of antecedent SMAP satellite soil moisture, radar rainfall and MODIS vegetation on runoff production in an agricultural region. *J. Hydrol.* **2019**, *579*, 124210. [CrossRef]
19. Draper, C.; Mahfouf, J.-F.; Calvet, J.-C.; Martin, E.; Wagner, W. Assimilation of ASCAT near-surface soil moisture into the SIM hydrological model over France. *Hydrol. Earth Syst. Sci.* **2011**, *15*, 3829–3841. [CrossRef]
20. Brocca, L.; Moramarco, T.; Melone, F.; Wagner, W.; Hasenauer, S.; Hahn, S. Assimilation of surface- and root-zone ASCAT soil moisture products into rainfallrunoff modeling. *IEEE Trans. Geosci. Remote Sens.* **2012**, *50*, 2542–2555. [CrossRef]
21. Massari, C.; Brocca, L.; Tarpanelli, A.; Moramarco, T. Data assimilation of satellite soil moisture into rainfall-runoff modelling: A complex recipe? *Remote Sens.* **2015**, *7*, 11403–11433. [CrossRef]
22. Meng, S.; Xie, X.; Liang, S. Assimilation of soil moisture and streamflow observations to improve flood forecasting with considering runoff routing lags. *J. Hydrol.* **2017**, *550*, 568–579. [CrossRef]
23. Loizu, J.; Massari, C.; Álvarez-Mozos, J.; Tarpanelli, A.; Brocca, L.; Casalí, J. On the assimilation set-up of ASCAT soil moisture data for improving streamflow catchment simulation. *Adv. Water Resour.* **2018**, *111*, 86–104. [CrossRef]
24. Ciupak, M.; Ozga-Zielinski, B.; Adamowski, J.; Deo, R.C.; Kochanek, K. Correcting satellite precipitation data and assimilating satellite-derived soil moisture data to generate ensemble hydrological forecasts within the hbv rainfall-runoff model. *Water* **2019**, *11*, 2138. [CrossRef]
25. Parajka, J.; Naeimi, V.; Blöschl, G.; Komma, J. Matching ERS scatterometer based soil moisture patterns with simulations of a conceptual dual layer hydrologic model over Austria. *Hydrol. Earth Syst. Sci.* **2009**, *13*, 259–271. [CrossRef]
26. Wanders, N.; Bierkens, M.F.P.; de Jong, S.M.; de Roo, A.; Karssenberg, D. The benefits of using remotely sensed soil moisture in parameter identification of large-scale hydrological models. *Water Resour. Res.* **2014**, *50*, 6874–6891. [CrossRef]
27. Rajib, A.; Merwade, V.; Yu, Z. Multi-objective calibration of a hydrologic model using spatially distributed remotely sensed/in-situ soil moisture. *J. Hydrol.* **2016**, *536*, 192–207. [CrossRef]
28. Kundu, D.; Vervoort, R.; van Ogtrop, F. The value of remotely sensed surface soil moisture for model calibration using SWAT. *Hydrol. Process.* **2017**, *31*, 2764–2780. [CrossRef]
29. Li, Y.; Grimaldi, S.; Pauwels, V.; Walker, J. Hydrologic model calibration using remotely sensed soil moisture and discharge measurements: The impact on predictions at gauged and ungauged locations. *J. Hydrol.* **2018**, *557*, 897–909. [CrossRef]
30. Xiong, L.; Zeng, L. Impacts of introducing remote sensing soil moisture in calibrating a distributed hydrological model for streamflow simulation. *Water* **2019**, *11*, 666. [CrossRef]
31. Parajka, J.; Merz, R.; Blöschl, G. Uncertainty and multiple objective calibration in regional water balance modelling: Case study in 320 Austrian catchments. *Hydrol. Process.* **2007**, *21*, 435–446. [CrossRef]
32. Sutanudjaja, E.H.; van Beek, L.P.H.; de Jong, S.M.; van Geer, F.C.; Bierkens, M.F.P. Calibrating a large-extent high-resolution coupled groundwater-land surface model using soil moisture and discharge data. *Water Resour. Res.* **2014**, *50*, 687–705. [CrossRef]
33. Kunnath-Poovakka, A.; Ryu, D.; Renzullo, L.; George, B. The efficacy of calibrating hydrologic model using remotely sensed evapotranspiration and soil moisture for streamflow prediction. *J. Hydrol.* **2016**, *535*, 509–524. [CrossRef]
34. López, P.L.; Sutanudjaja, E.H.; Schellekens, J.; Sterk, G.; Bierkens, M.F.P. Calibration of a large-scale hydrological model using satellite-based soil moisture and evapotranspiration products. *Hydrol. Earth Syst. Sci.* **2017**, *21*, 3125–3144. [CrossRef]
35. Nijzink, R.C.; Almeida, S.; Pechlivanidis, I.G.; Capell, R.; Gustafssons, D.; Arheimer, B.; Parajka, J.; Freer, J.; Han, D.; Wagener, T.; et al. Constraining conceptual hydrological models with multiple information sources. *Water Resour. Res.* **2018**, *54*, 8332–8362. [CrossRef]
36. Demirel, M.C.; Özen, A.; Orta, S.; Toker, E.; Demir, H.K.; Ekmekcioğlu, Ö.; Tayşi, H.; Eruçar, S.; Sağ, A.B.; Sari, Ö.; et al. Additional value of using satellite-based soil moisture and two sources of groundwater data for hydrological model calibration. *Water* **2019**, *11*, 2083. [CrossRef]
37. Széles, B.; Parajka, J.; Hogan, P.; Silasari, R.; Pavlin, L.; Strauss, P.; Blöschl, G. The added value of different data types for calibrating and testing a hydrologic model in a small catchment. *Water Resour. Res.* **2020**, *56*, e2019WR026153. [CrossRef]
38. Sleziak, P.; Szolgay, J.; Hlavčová, K.; Deutemanm, D.; Parajka, J.; Danko, M. Factors controlling alternations in the performance of a runoff model in changing climate conditions. *J. Hydrol. Hydromech.* **2018**, *66*, 381–392. [CrossRef]
39. Zhang, Y.; Schaap, M.G.; Zha, Y. A high-resolution global map of soil hydraulic properties produced by a hierarchical parameterization of a physically based water retention model. *Water Resour. Res.* **2018**, *54*, 9774–9790. [CrossRef]
40. Hengl, T.; de Jesus, J.M.; MacMillan, R.A.; Batjes, N.H.; Heuvelink, G.B.M.; Ribeiro, E.; Samuel-Rosa, A.; Kempen, B.; Leenaars, J.G.B.; Walsh, M.G.; et al. SoilGrids1km—Global soil information based on automated mapping. *PLoS ONE* **2014**, *9*, e105992. [CrossRef]
41. Hiebl, J.; Frei, C. Daily temperature grids for Austria since 1961—Concept, creation and applicability. *Theor. Appl. Clim.* **2016**, *124*, 161–178. [CrossRef]

42. Parajka, J.; Merz, R.; Blöschl, G. A comparison of regionalisation methods for catchment model parameters. *Hydrol. Earth Syst. Sci.* **2005**, *9*, 157–171. [CrossRef]
43. Hiebl, J.; Frei, C. Daily precipitation grids for Austria since 1961—Development and evaluation of a spatial dataset for hydroclimatic monitoring and modelling. *Theor. Appl. Clim.* **2017**, *132*, 327–345. [CrossRef]
44. Hahn, S.; Wagner, W.; Steele-Dunne, S.C.; Vreugdenhil, M.; Melzer, T. Improving ASCAT soil moisture retrievals with an enhanced spatially variable vegetation parameterization. *IEEE Trans. Geosci. Remote Sens.* **2021**, *59*, 8241–8256. [CrossRef]
45. Pfeil, I.; Vreugdenhil, M.; Hahn, S.; Wagner, W.; Strauss, P.; Blöschl, G. Improving the seasonal representation of ASCAT soil moisture and vegetation dynamics in a temperate climate. *Remote Sens.* **2018**, *10*, 1788. [CrossRef]
46. Wagner, W.; Lemoine, G.; Borgeaud, M.; Rott, H. A study of vegetation cover effects on ERS scatterometer data. *IEEE Trans. Geosci. Remote Sens.* **1999**, *37*, 938–948. [CrossRef]
47. Albergel, C.; Rüdiger, C.; Pellarin, T.; Calvet, J.-C.; Fritz, N.; Froissard, F.; Suquia, D.; Petitpa, A.; Piguet, B.; Martin, E. From near-surface to root-zone soil moisture using an exponential filter: An assessment of the method based on in-situ observations and model simulations. *Hydrol. Earth Syst. Sci.* **2008**, *12*, 1323–1337. [CrossRef]
48. Mullen, K.M.D.; Gil, D.; Windover, D.; Cline, J. DEoptim: An R package for global optimalization by differential evolution. *J. Stat. Softwre* **2011**, *40*, 1–26.
49. Nash, J.; Sutcliffe, J. River flow forecasting through conceptual models part I—A discussion of principles. *J. Hydrol.* **1970**, *10*, 282–290. [CrossRef]
50. Sleziak, P.; Szolgay, J.; Hlavčová, K.; Danko, M.; Parajka, J. The effect of the snow weighting on the temporal stability of hydrologic model efficiency and parameters. *J. Hydrol.* **2020**, *583*, 124639. [CrossRef]
51. Dumont, M.; Gascoin, S. Optical remote sensing of snow cover. *Land Surf. Remote Sens. Cont. Hydrol.* **2016**, 115–137. [CrossRef]
52. Xu, X.; Li, J.; Tolson, B.A. Progress in integrating remote sensing data and hydrologic modeling. *Prog. Phys. Geogr. Earth Environ.* **2014**, *38*, 464–498. [CrossRef]